Electronic Supplementary Material (ESI) for Journal of Materials Chemistry A.

Supporting Information

Molecular Blends of Methylated-Poly(ethylenimine) and Amorphous Porous Organic Cages for SO_2 Removal

Guanghui Zhu[1,#], Jan-Michael Y. Carrillo[2,3,#], Achintya Sujan[1], Claudia N. Okonkwo[1], Sangjae Park[1], Bobby G. Sumpter[2,3,*], Christopher W. Jones[1,*], Ryan P. Lively[1,*]

1. School of Chemical & Biomolecular Engineering, Georgia Institute of Technology, Atlanta, Georgia 30332, United States

2. Center for Nanophase Materials Sciences, Oak Ridge National Laboratory, Oak Ridge, Tennessee 37831, United States

3. Computational Sciences and Engineering Division, Oak Ridge National Laboratory, Oak Ridge, Tennessee 37831, United States

Details of Molecular Dynamics Simulations

To simulate the structure of the aminopolymer/ASPOC composites, we performed isobaric-isothermal (NPT) ensemble and canonical (NVT) ensemble all atomistic molecular dynamics (AMD). The force field used in the simulations was the Generalized Amber Force Field (GAFF)[1] and the atomic partial charges were derived from the AM1/BCC routine in Antechamber,[2] which is a part of the AMBER package. The total potential energy in GAFF is,

$$U_{tot} = \sum_{bonds} k_{bond}\left(r - r_{eq}\right)^2 + \sum_{angles} k_{angle}\left(\theta - \theta_{eq}\right)^2 + \sum_{dihedrals} k_{dihedral}\left(1 + d\cos(n\phi)\right) + \sum_{1<j}\left[\frac{A_{ij}}{R_{ij}^{12}} - \frac{B_{ij}}{R_{ij}^{6}} + \frac{q_i q_j}{\varepsilon R_{ij}}\right]$$

where r_{eq} and θ_{eq} are equilibrium structural parameters; k_{bond}, k_{angle} and $k_{dihedral}$ are force constants; n and d are dihedral angle parameters; and A, B, q and ε are parameters that characterize the non-bonded interactions. The Particle-Particle-Particle-Mesh (PPPM)[3] method with an accuracy of 1.0×10^{-4} and near-field cutoff set to 10.0 Å was used to account for contributions from the long-range electrostatic interactions. The equations of motion in the AMD simulations were integrated by using the velocity Verlet algorithm with a time step of 1.0 fs. All simulations were performed using LAMMPS software package.[4, 5] Although a cage specific force-field has been developed,[6] we opted for the more general force-field, GAFF, since we wanted the same level of accuracy in modeling PEI and mPEI as with the POC's. We expect GAFF is capable of adequately describing the structure of the cages and polymers since GAFF is known to model hydrocarbons reasonably well.

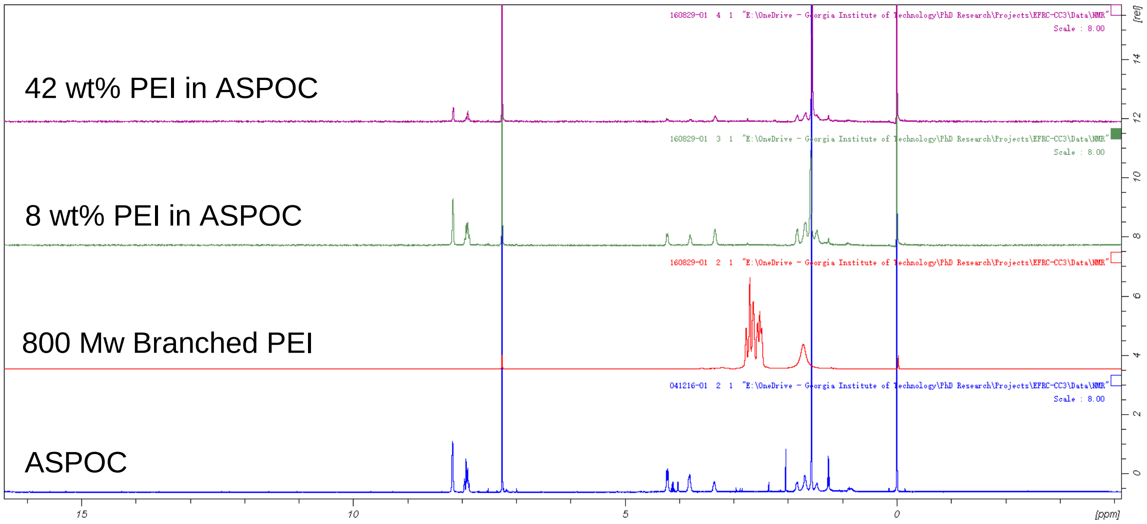

Figure S1. ^{1}H NMR spectra of ASPOC, PEI, and two mixtures of ASPOC and PEI. The spectra for the mixtures show no signs of PEI protons, indicating reaction between PEI and ASPOC to form insoluble polymers.

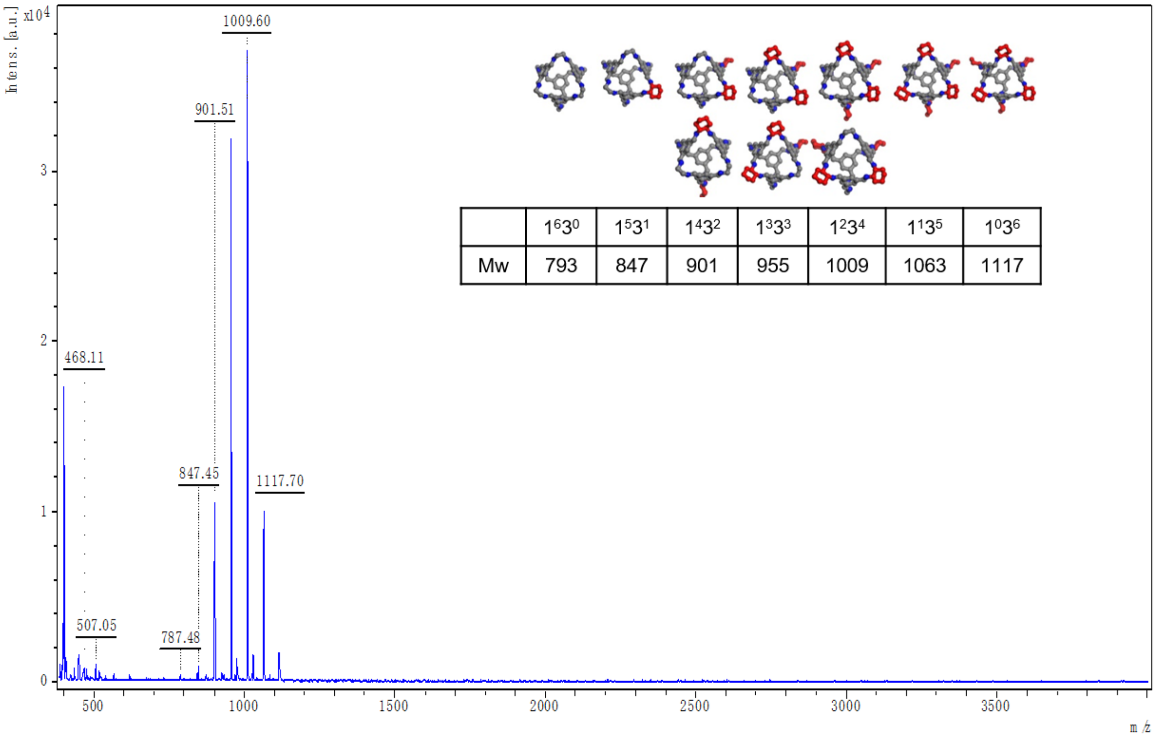

	$1^6 3^0$	$1^5 3^1$	$1^4 3^2$	$1^3 3^3$	$1^2 3^4$	$1^1 3^5$	$1^0 3^6$
Mw	793	847	901	955	1009	1063	1117

Figure S2. MALDI-MS spectrum of 42 wt % PEI in ASPOC. Only peaks corresponding to cage mixtures are observed in the spectrum, agreeing with the NMR results.

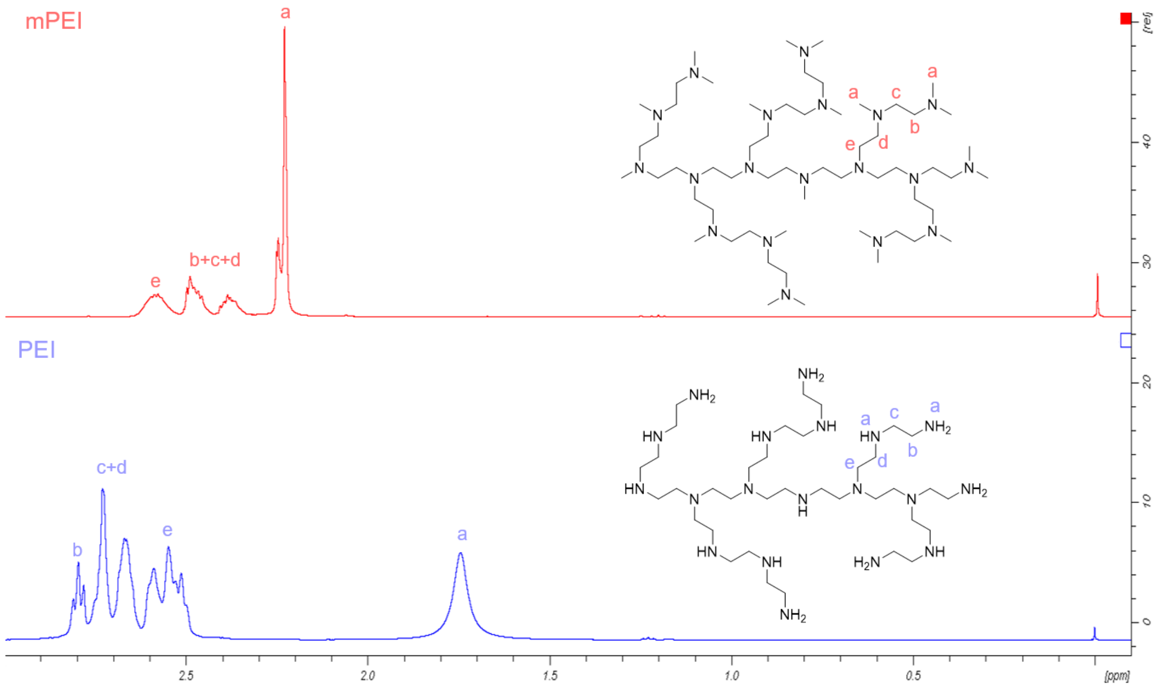

Figure S3. ^{1}H NMR spectra of PEI and mPEI.

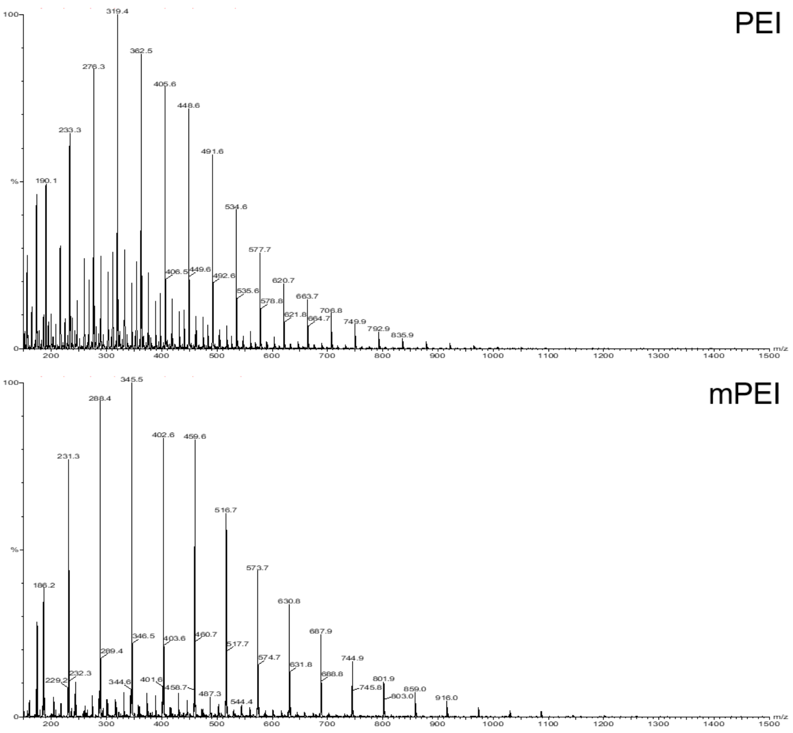

N unit	PEI Mw	mPEI Mw
2	60.07	116.13
3	103.11	173.19
4	146.15	230.25
5	189.2	287.3
6	232.24	344.36
7	275.28	401.42
8	318.32	458.48
9	361.36	515.54
10	404.41	572.59
11	447.45	629.65
12	490.49	686.71
13	533.53	743.77
14	576.58	800.83
15	619.62	857.88
16	662.66	914.94
17	705.7	972
18	748.74	1029.06
19	791.79	1086.11

Figure S4. ESI-MS spectra of PEI and mPEI.

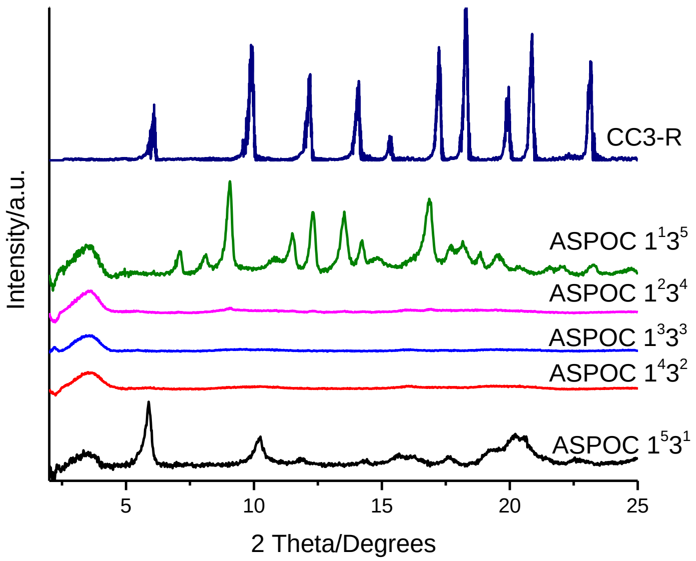

Figure S5. XRD patterns of ASPOC samples with different starting linker ratio.

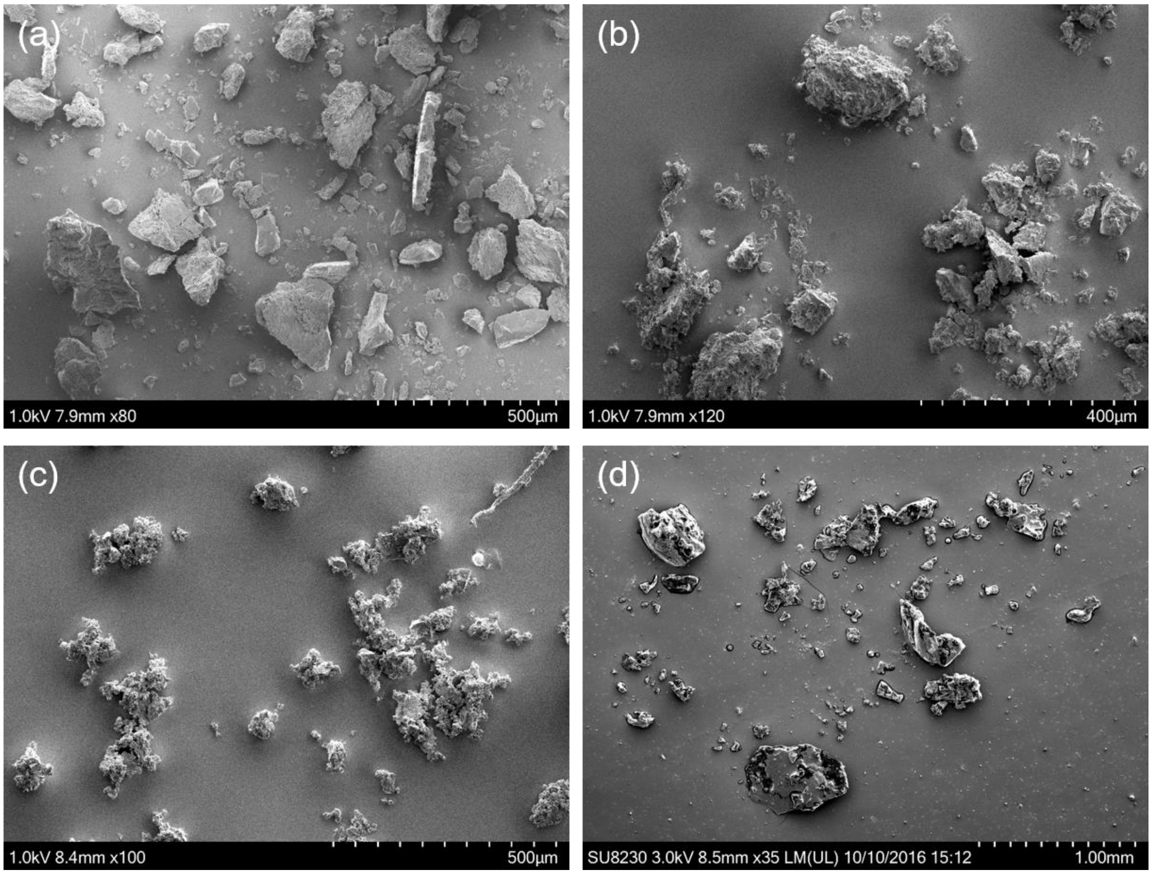

Figure S6. SEM of mPEI/ASPOC composite samples with different mPEI loading: (a) 10-mPEI/ASPOC, (b) 20-mPEI/ASPOC, (c) 40-mPEI/ASPOC, and (d) 80-mPEI/ASPOC.

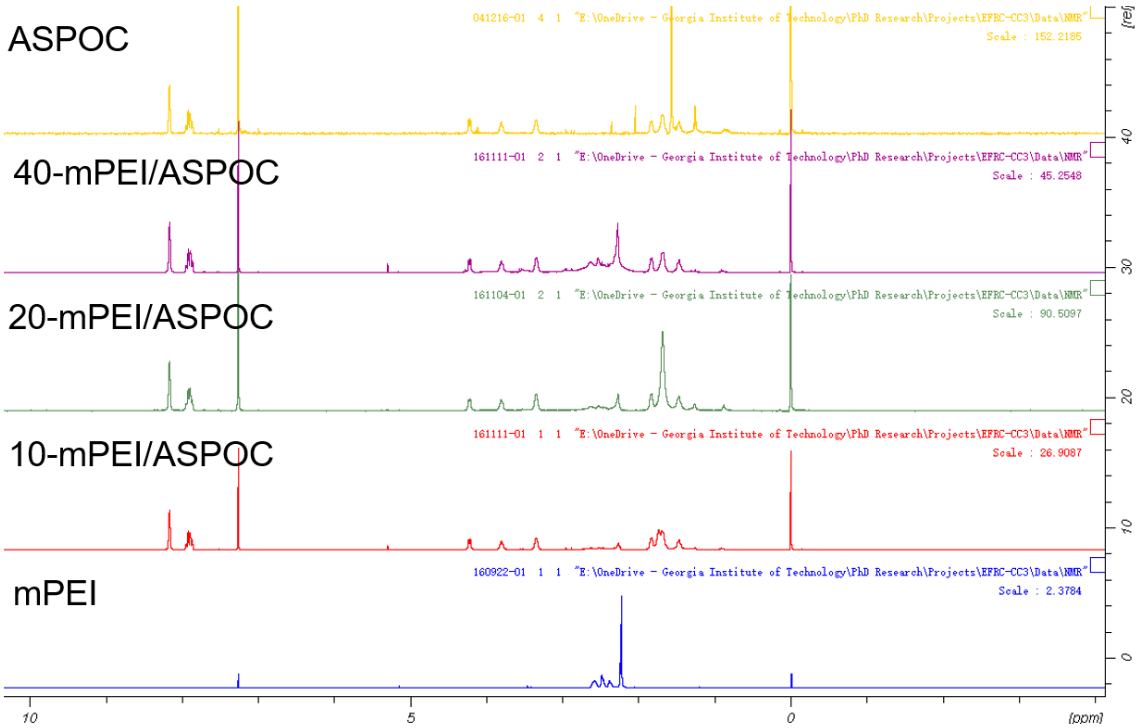

Figure S7. ^{1}H NMR of pure ASPOC, mPEI and three composite samples.

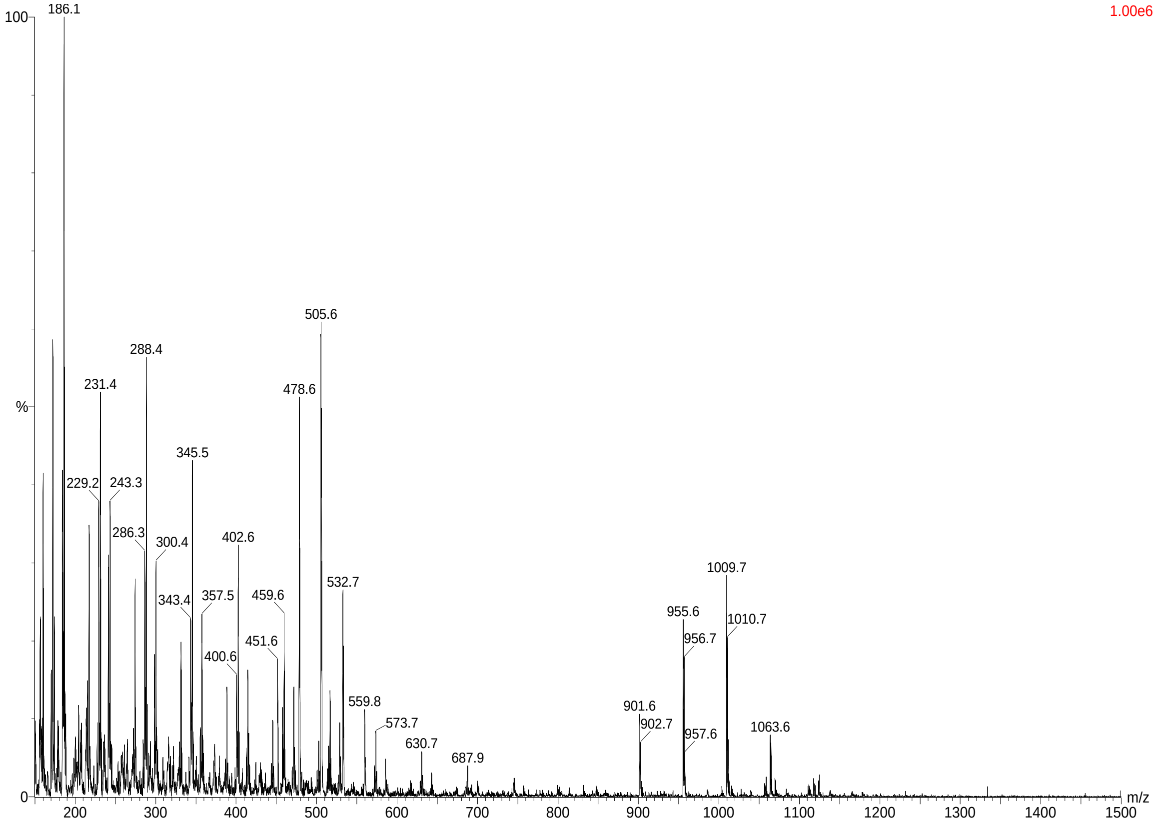

Figure S8. ESI-MS spectrum of 20-mPEI/ASPOC sample. Peaks in the left region correspond to mPEI molecules, peaks from 900-1200 m/z correspond to cage molecules.

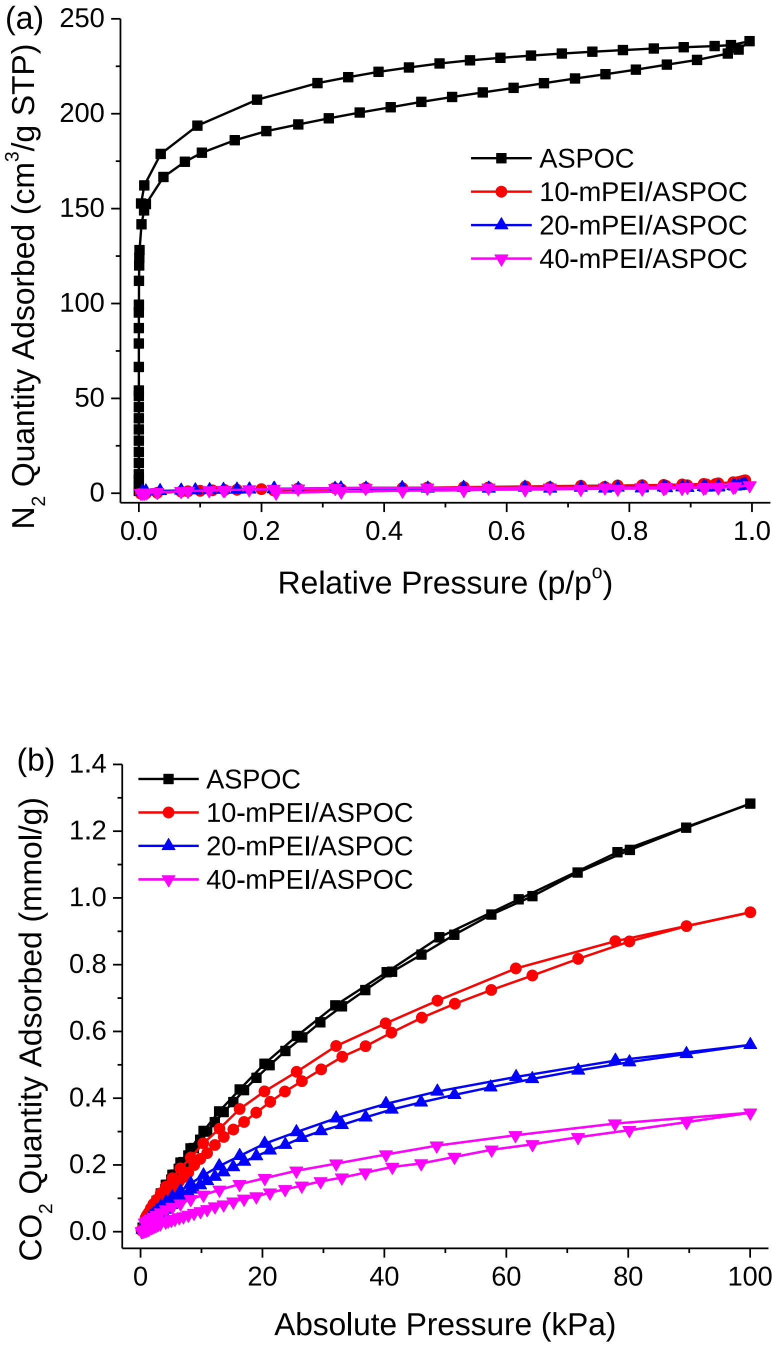

Figure S9. N_2 and CO_2 physisorption isotherms measured at 77 K and 308 K, respectively.

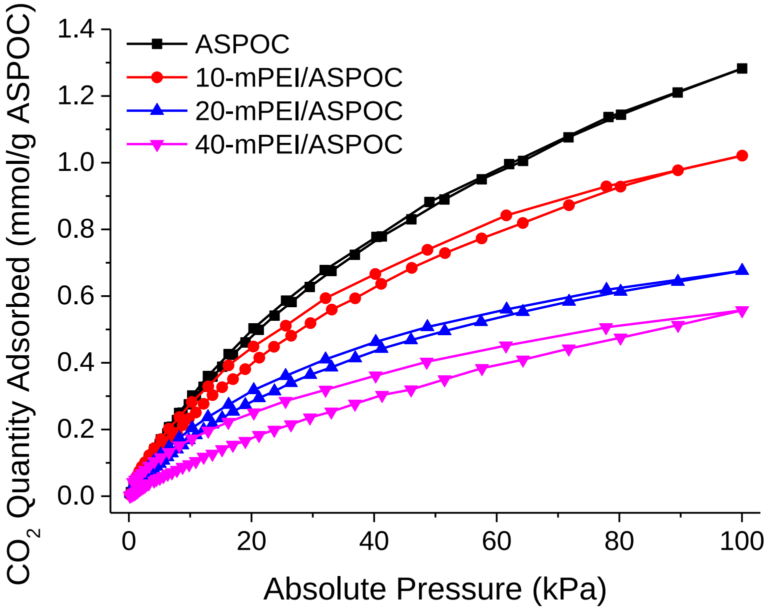

Figure S10. CO_2 physisorption isotherms normalized to ASPOC content based on elemental analysis.

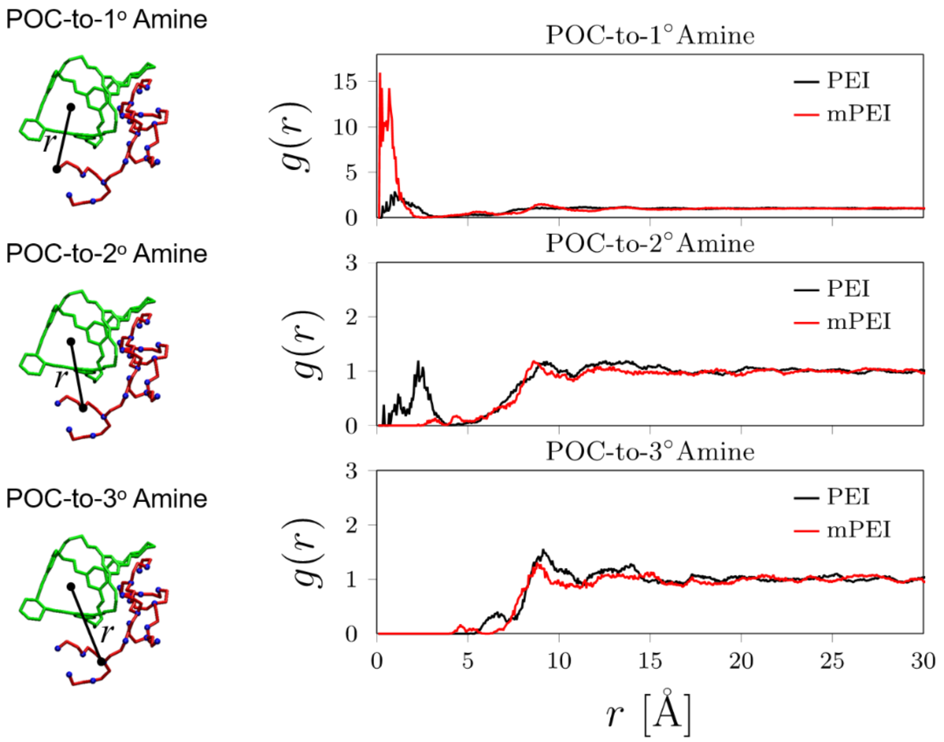

Figure S11. Partial radial distribution functions g(r) of the distance, r, which denotes the distance between the center-of-mass position between ASPOC molecules (a) and between the nitrogen atoms of amines in 26.5% wt PEI or 26.3% wt mPEI composites (b). The images in the left depict the different definitions of r where blue dots in the polymer represents the location of the nitrogen atoms.

Table S1. Elemental analysis data for ASPOC and composite materials (wt%)

	C	H	N
ASPOC	74.29	7.06	16.6
mPEI	60.56	12.53	23.16
10-mPEI/ASPOC	72.7	7.55	16.61
20-mPEI/ASPOC	70.37	8.08	16.84
40-mPEI/ASPOC	65.69	8.72	17.52

Table S2. Theoretical and calculated mPEI loadings in composite materials.

	ASPOC	10-mPEI/ASPOC	20-mPEI/ASPOC	40-mPEI/ASPOC	mPEI
Theoretical mPEI loading (wt%)	0	10	20	40	100
mPEI loading from elemental analysis (wt%)	0	6.3	17.2	36.0	100
N from mPEI (mmol/g)	0	1.09	2.96	6.18	17.19

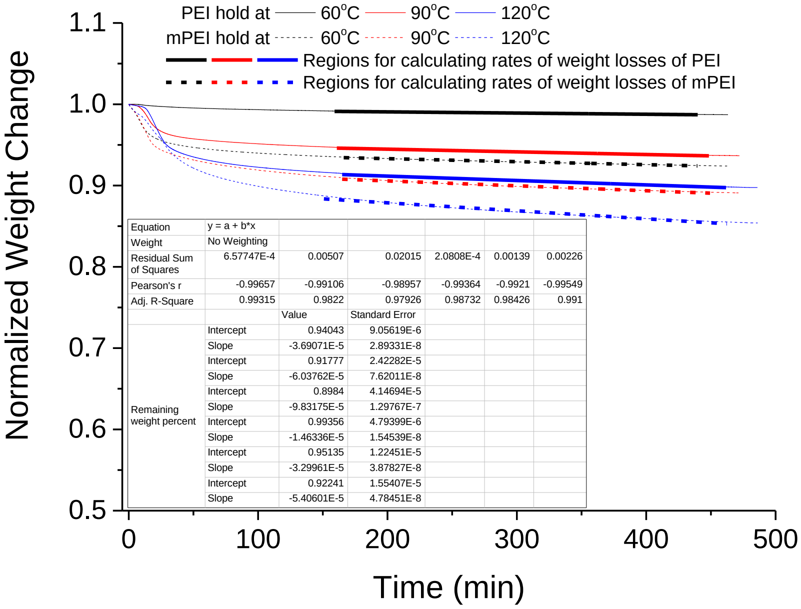

Equation	y = a + b*x					
Weight	No Weighting					
Residual Sum of Squares	6.57747E-4	0.00507	0.02015	2.0808E-4	0.00139	0.00226
Pearson's r	-0.99657	-0.99106	-0.98957	-0.99364	-0.9921	-0.99549
Adj. R-Square	0.99315	0.9822	0.97926	0.98732	0.98426	0.991
		Value	Standard Error			
Remaining weight percent	Intercept	0.94043	9.05619E-6			
	Slope	-3.69071E-5	2.89331E-8			
	Intercept	0.91777	2.42282E-5			
	Slope	-6.03762E-5	7.62011E-8			
	Intercept	0.8984	4.14694E-5			
	Slope	-9.83175E-5	1.29767E-7			
	Intercept	0.99356	4.79399E-6			
	Slope	-1.46336E-5	1.54539E-8			
	Intercept	0.95135	1.22451E-5			
	Slope	-3.29961E-5	3.87827E-8			
	Intercept	0.92241	1.55407E-5			
	Slope	-5.40601E-5	4.78451E-8			

Figure S12. Thermal stability of the PEI and mPEI at 60 °C, 90 °C, and 120 °C and the fitting parameters for calculating the rates of weight loses.

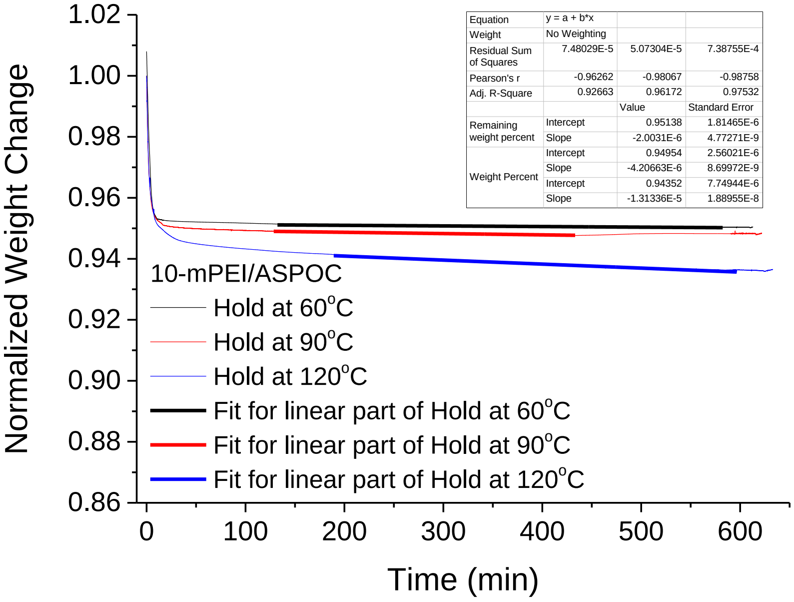

Equation	y = a + b*x		
Weight	No Weighting		
Residual Sum of Squares	7.48029E-5	5.07304E-5	7.38755E-4
Pearson's r	-0.96262	-0.98067	-0.98758
Adj. R-Square	0.92663	0.96172	0.97532
		Value	Standard Error
Remaining weight percent	Intercept	0.95138	1.81465E-6
	Slope	-2.0031E-6	4.77271E-9
Weight Percent	Intercept	0.94954	2.56021E-6
	Slope	-4.20663E-6	8.69972E-9
	Intercept	0.94352	7.74944E-6
	Slope	-1.31336E-5	1.88955E-8

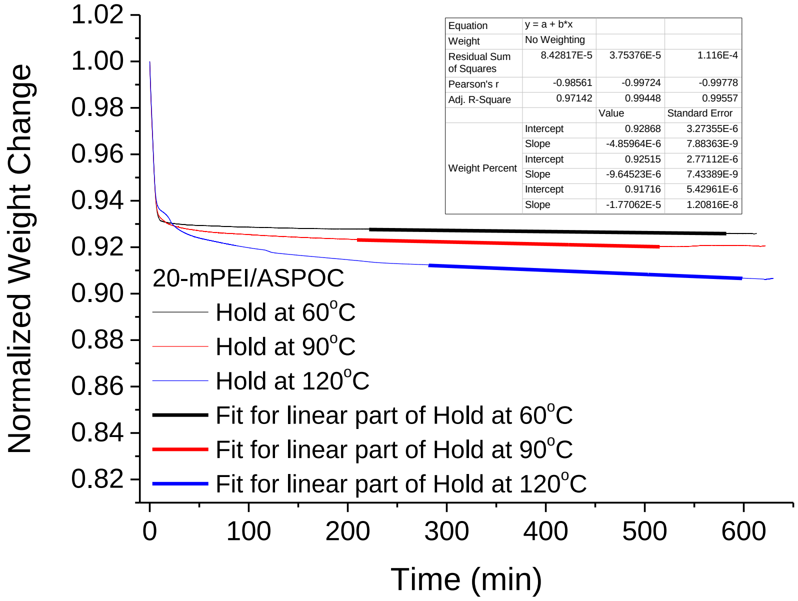

Equation	y = a + b*x		
Weight	No Weighting		
Residual Sum of Squares	8.42817E-5	3.75376E-5	1.116E-4
Pearson's r	-0.98561	-0.99724	-0.99778
Adj. R-Square	0.97142	0.99448	0.99557
		Value	Standard Error
Weight Percent	Intercept	0.92868	3.27355E-6
	Slope	-4.85964E-6	7.88363E-9
	Intercept	0.92515	2.77112E-6
	Slope	-9.64523E-6	7.43389E-9
	Intercept	0.91716	5.42961E-6
	Slope	-1.77062E-5	1.20816E-8

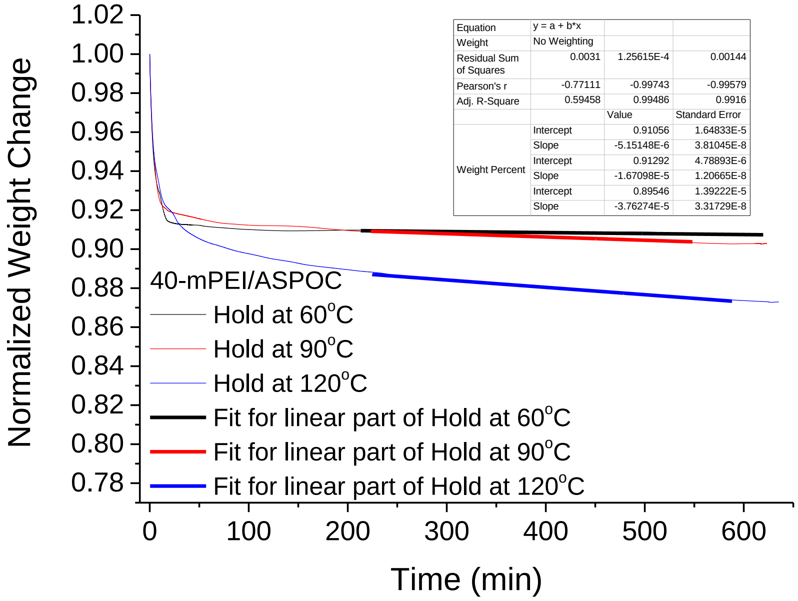

Equation	y = a + b*x		
Weight	No Weighting		
Residual Sum of Squares	0.0031	1.25615E-4	0.00144
Pearson's r	-0.77111	-0.99743	-0.99579
Adj. R-Square	0.59458	0.99486	0.9916
		Value	Standard Error
Weight Percent	Intercept	0.91056	1.64833E-5
	Slope	-5.15148E-6	3.81045E-8
	Intercept	0.91292	4.78893E-6
	Slope	-1.67098E-5	1.20665E-8
	Intercept	0.89546	1.39222E-5
	Slope	-3.76274E-5	3.31729E-8

Figure S13. Thermal stability of the composite materials hold at 60 °C, 90 °C, and 120 °C and the fitting parameters for calculating the rates of weight loses.

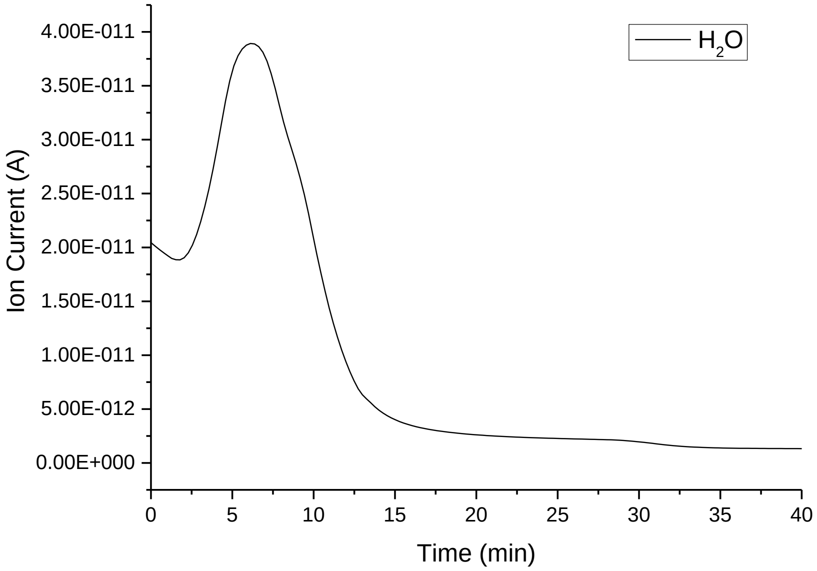

Figure S14. Desorption of water from 20-mPEI/ASPOC indicated by online mass spectrometry ion current change during heating to 90ºC with 10 ºC/min and then cooled down to room temperature from 30 min.

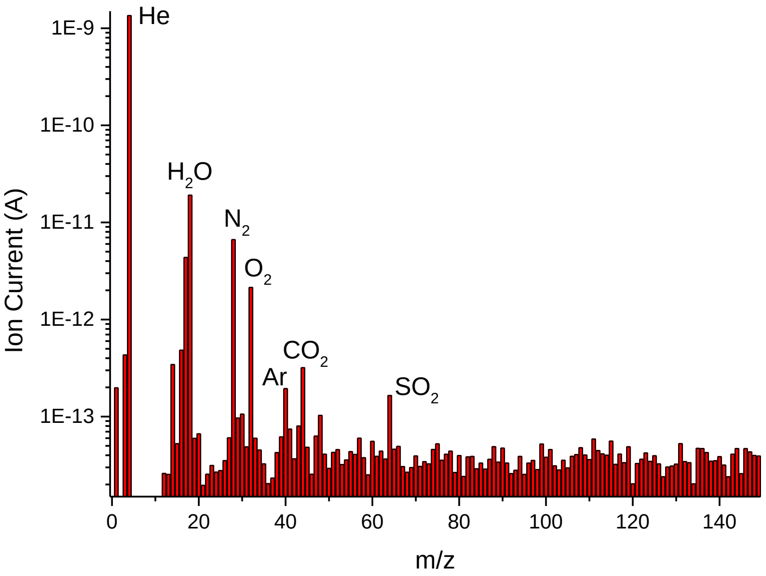

Figure S15. Selected mass spectrometry bar-graph during desorption of 20-mPEI/ASPOC between 0-150 m/z.

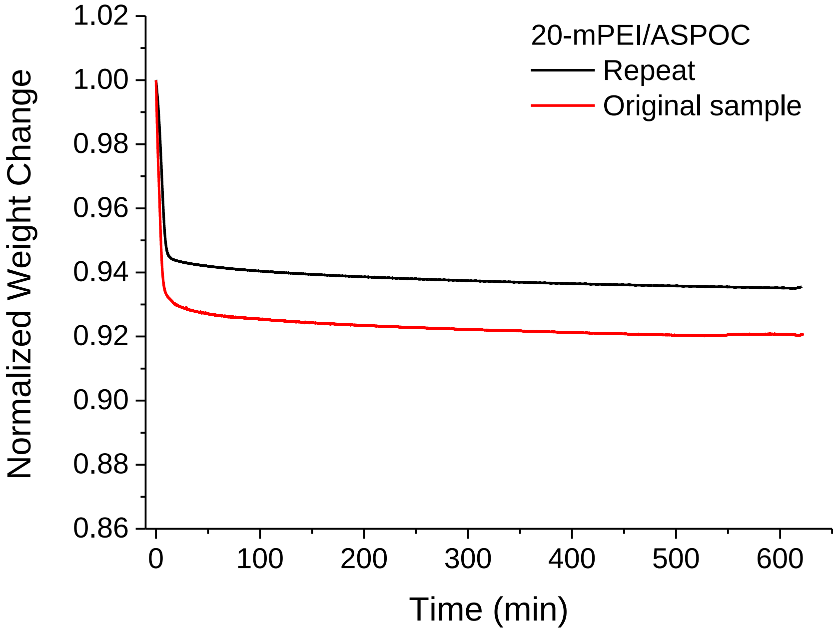

Figure S16. Weight loss profile of 20-mPEI/ASPOC after drying and re-exposure to air for 5 days. Compared to the weight loss of the fresh sample, the weight loss is reduced in shorter air exposure time case, which supports our hypothesis that the initial mass loss can be attributed to sorbed water.

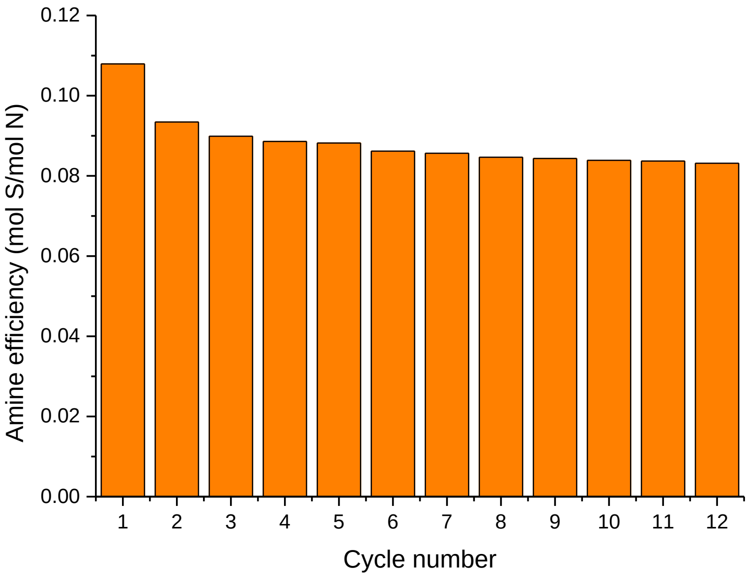

Figure S17. Amine efficiency of 20-mPEI/ASPOC for 12 cycles.

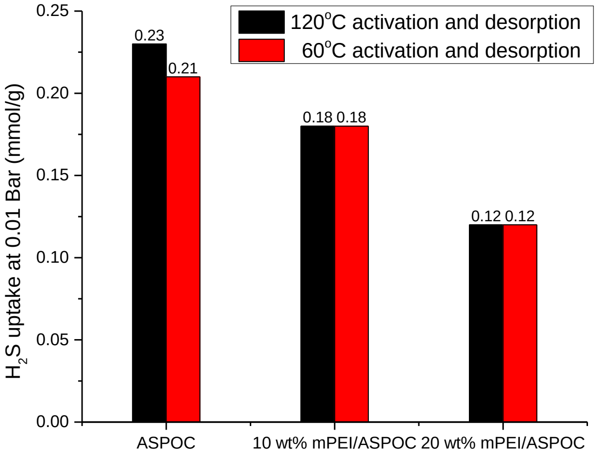

Figure S18. H_2S adsorption into ASPOC.

Although mPEI is not active for chemisorption of H_2S, we tested the adsorption of H_2S into the ASPOC as well as the composite materials. Similar to CO_2 adsorption in the materials, a general decreasing trend was found with H_2S adsorption determined gravimetrically. Although mPEI did not facilitate the adsorption of H_2S, rapid and stable adsorption of H_2S into the ASPOC was observed. This indicates the potential of ASPOCs as a selective H_2S adsorbent by itself or it can be used as a stable support for other H_2S sorbents.

References

1. J. Wang, R. M. Wolf, J. W. Caldwell, P. A. Kollman and D. A. Case, *J. Comput. Chem.*, 2004, **25**, 1157-1174.
2. J. Wang, W. Wang, P. A. Kollman and D. A. Case, *J. Am. Chem. Soc*, 2001, **222**, U403.

3. R. W. Hockney and J. W. Eastwood, *Computer simulation using particles*, crc Press, 1988.
4. S. Plimpton, *J. Comput. Phys.*, 1995, **117**, 1-19.
5. W. M. Brown, P. Wang, S. J. Plimpton and A. N. Tharrington, *Comput. Phys. Commun.*, 2011, **182**, 898-911.
6. D. Holden, K. E. Jelfs, A. I. Cooper, A. Trewin and D. J. Willock, *J. Phys. Chem. C*, 2012, **116**, 16639-16651.